EUR 595.e

EUROPEAN ATOMIC ENERGY COMMUNITY - EURATOM

INTERPRETATION AND EVALUATION OF NON-IDEAL GAS RELEASE IN POST-ACTIVATION MEASUREMENTS (Rare-Gas Diffusion in Solids 11)

by

T. LAGERWALL and P. SCHMELING

1964

EURATOM / UNITED STATES Agreement for Cooperation

EURAEC Report No 806
prepared by Hahn-Meitner-Institut für Kernforschung - Berlin, W. Germany

Euratom Contract No 094-62-9 RDD

LEGAL NOTICE

This document was prepared under the sponsorship of the Commission of the European Atomic Energy Community (EURATOM) in pursuance of the joint program laid down by the Agreement for Cooperation signed on 8 November 1958 between the Government of the United States of America and the European Atomic Energy Community.

It is specified that neither the Euratom Commission, nor the Government of the United States, their contractors or any person acting on their behalf :

1° — Makes any warranty or representation, express or implied, with respect to the accuracy, completeness, or usefulness of the information contained in this document, or that the use of any information, apparatus, method, or process disclosed in this document may not infringe privately owned rights ; or

2° — Assumes any liability with respect to the use of, or for damages resulting from the use of any information, apparatus, method or process disclosed in this document.

This report can be obtained, at the price of Belgian Francs 70,— from : PRESSES ACADEMIQUES EUROPEENNES — 98, Chaussée de Charleroi, Brussels 6.

Please remit payments to :

— BANQUE DE LA SOCIETE GENERALE (Agence Ma Campagne) — Brussels — account No 964.558,

— BELGIAN AMERICAN BANK AND TRUST COMPANY — New York — account No 121.86,

— LLOYDS BANK (Foreign) Ltd. — 10 Moorgate — London E.C.2,

giving the reference : « EUR 595 . e — INTERPRETATION AND EVALUATION OF NON-IDEAL GAS RELEASE IN POST-ACTIVATION MEASUREMENTS ».

This document was duplicated on the basis of the best available copy.

Printed by L. VANMELLE S.A., GHENT
Brussels, February 1964

EUR 595.e

INTERPRETATION AND EVALUATION OF NON-IDEAL GAS RELEASE IN POST-ACTIVATION MEASUREMENTS
by T. LAGERWALL and P. SCHMELING

European Atomic Energy Community — EURATOM
Euratom/United States Agreement for Cooperation
EURAEC Report No 806 prepared by Hahn-Meitner-Institut für Kernforschung, Berlin (W. Germany)
Euratom Contract No 094-62-9 RDD
Brussels, February 1964 — 51 pages — 28 figures

This report gives a review of possible causes of the non-ideal gas release kinetics often observed in post-activation diffusion experiments. It is pointed out, that in the calculation of diffusion coefficients from the corresponding release curves, D-values which may be different by orders of magnitude will come out, depending on different interpretation of the experimental curve. This may

EUR 595.e

INTERPRETATION AND EVALUATION OF NON-IDEAL GAS RELEASE IN POST-ACTIVATION MEASUREMENTS
by T. LAGERWALL and P. SCHMELING

European Atomic Energy Community — EURATOM
Euratom/United States Agreement for Cooperation
EURAEC Report No 806 prepared by Hahn-Meitner-Institut für Kernforschung, Berlin (W. Germany)
Euratom Contract No 094-62-9 RDD
Brussels, February 1964 — 51 pages — 28 figures

This report gives a review of possible causes of the non-ideal gas release kinetics often observed in post-activation diffusion experiments. It is pointed out, that in the calculation of diffusion coefficients from the corresponding release curves, D-values which may be different by orders of magnitude will come out, depending on different interpretation of the experimental curve. This may

contribute to the uncommonly broad scattering of the values of diffusion coefficients found in the literature and shows that a deeper insight of the underlying physical processes is needed in order to evaluate the experimental data correctly. On discussing present experimental results, different assumptions regarding the nature of these processes are made, and the consequences for the experimentally observed release patterns are discussed. Recommendations are given for the evaluation of complicated release curves.

contribute to the uncommonly broad scattering of the values of diffusion coefficients found in the literature and shows that a deeper insight of the underlying physical processes is needed in order to evaluate the experimental data correctly. On discussing present experimental results, different assumptions regarding the nature of these processes are made, and the consequences for the experimentally observed release patterns are discussed. Recommendations are given for the evaluation of complicated release curves.

EUR 595.e

EUROPEAN ATOMIC ENERGY COMMUNITY - EURATOM

INTERPRETATION AND EVALUATION OF NON-IDEAL GAS RELEASE IN POST-ACTIVATION MEASUREMENTS (Rare-Gas Diffusion in Solids 11)

by

T. LAGERWALL and P. SCHMELING

1964

EURATOM / UNITED STATES Agreement for Cooperation

EURAEC Report No 806
prepared by Hahn-Meitner-Institut für Kernforschung - Berlin, W. Germany

Euratom Contract No 094-62-9 RDD

CONTENTS

		Page
	Introduction	5
1	Time-dependent diffusion coefficient	6
2	Trapping and condensation in the lattice	8
3	Surface effects	13
4	Powders and polycrystalline materials	17
	4.1 Influence of grain size	17
	4.2 Influence of grain size distribution	17
	4.3 Pore desorption and grain boundary diffusion	18
	4.4 Sintering and grain growth	19
5	Other causes to non-ideal release	21
	5.1 Phase transformations during the annealing process	21
	5.2 Chemical reaction of the specimen during the PAD annealing process	22
	5.3 Evaporation of the specimen during the annealing process	23
	5.4 Changed concentration profile due to flux depression	28
6	Notes on the evaluation of non-ideal release curves	29
	6.1 Introduction	29
	6.2 Time-dependent diffusion coefficient	29
	6.3 The case of overlapping processes	32
	6.4 The case of competing processes	34
	6.5 Conclusions	34
	6.6 Recommendations for the evaluation of release curves	35
	Acknowledgement	37
	References	37
	Figures	43 ff

INTRODUCTION

Investigations by various authors on the transport of fission rare-gases in reactor materials exhibit an obvious scatter of diffusion coefficients. Though this can be partly explained as being caused by the varying structural properties of the material used, it is greatly influenced by the fact that the release kinetics normally does not follow the ideal diffusion behaviour. This may make the normal evaluation methods inappropriate and, as a consequence, lead to diffusion coefficients which may be erroneous by orders of magnitude.

The fractional gas release, F, has often the form indicated in Figure 1. The first part of the curve, the slope of which has a large value, is normally referred to as an activity burst. Whatever may be the cause of this burst, it is evident that at least two processes must contribute to the form of the curve.

As there is very little experimental evidence on the nature of these processes, investigators are often inclined to regard curves of this type as normal for diffusion and calculate diffusion coefficients from the slope of the latter part of the curve. However, one has to understand the nature of the underlying processes which cause the deviation from diffusion kinetics if these have been established, it will in most cases be possible to evaluate the experiment quantitatively; if not, a quantitative evaluation of experimental results may be highly unreliable.

In the following the abbreviation PAD is used for post-activation diffusion and DAD for dum-activation or in-pile diffusion, cf. [5]. The references [1] to [10] refer to earlier publications of Zimen and co-workers on the subject of rare-gas diffusion in solids.*)

*) Note added in proof: The authors would like to draw attention to a Harwell report on a closely related theme.
Davies, Long: Abnormal kinetics in the release of inert gases from uranium dioxide, AERE-M969, May, 1963

1 TIME-DEPENDENT DIFFUSION COEFFICIENT*

Whenever the temperature of the specimen is changed during a PAD experiment, the diffusion coefficient D is, of course, also changed and may thus be regarded as time-dependent. The mathematical consequences of this is discussed in section 6.2, and it is pointed out that the correct evaluation should be made from an F^2-t-diagram, at least as long as ideal diffusion is observed. An F-$\sqrt{t}$-plot would introduce "evaluation bursts" whenever the temperature is increased (cf. Figure 21); such bursts have no physical reality.

Because of the fact that it always takes some time for the specimen to attain the anneal temperature, D has to be considered more or less time-dependent in every PAD experiment, depending on heating time and time of annealing. Initial deviations from the ideal linear relation of F versus t (see e.g. [11] may be due to this. The F-$\sqrt{t}$-curve will have a small negative or positive intercept with the F-axis depending on whether zero time is set corresponding to "temperature raised" or "temperature attained". It is likely that these deviations from ideal behaviour will disappear in an F^2-t-diagram, cf. Figure 2.

Since the rare-gas atoms are much larger than the ions of the host crystal, it is to be expected that their diffusion is very sensitive to the degree of disorder in the lattice; i.e., a vacancy rather than an interstitial-interstitial mechanism is assumed as a first hypothesis. Since the vacancy concentration in a neutron-irradiated crystal does not correspond to thermodynamical equilibrium but is much higher, the diffusion coefficient could be expected to have a larger value than in an unirradiated crystal. In a PAD experiment the radiation induced defects begin to heal out until ultimately their concentration is equal to the equilibrium concentration at the anneal temperature. This means that the diffusion coefficient is decreasing and thus time-dependent at the begin-

---

* cf. the general mathematical treatment of diffusion release with time-dependent diffusion coefficient by Gaus [6, 8]

ning of the anneal. If the commonly observed non-ideal behaviour (Figure 1) is interpreted in terms of a time-dependent diffusion coefficient, the slope of the latter part of the release curve in an F^2-t (not F-$\sqrt{t}$) diagram corresponds to the proper value of the diffusion coefficient at equilibrium.

Whether a burst due to non-equilibrium conditions as described above can actually be observed or not, depends on such factors as the total neutron exposure, the time required for the non-equilibrium defects to heal but, and the limit of detection of the measuring device.

An attempt to obtain deviations from ideal kinetics as a result of this mechanism was undertaken at this laboratory on the system CaF_2/Ar, for which the ideal kinetics is known to be valid at low irradiation doses [9]. It was found, however, that an increase of the neutron dose by a factor 10^3 did not cause any observable deviations of the diffusion kinetics. The release of argon was measured from single crystals which had been irradiated to an integrated fast flux of 10^{15}cm^{-2} [9] and 10^{18} cm^{-2} [12] respectively; the corresponding argon concentration was in both cases less than 10^{12} atoms/cm^3. Though the Frenkel defect concentration in the latter case roughly corresponds to the thermodynamical defect concentration at about 900°C,* no initial burst of activity was found even at temperatures as low as 700°C. On the contrary, the diffusion was s l o w e r than in the less irradiated crystals, and the values of D turned out to be lower within the whole range of temperatures. The difference is not appreciable at high temperatures but is of the order of several magnitudes at lower temperatures. Thus, the diffusion is not enhanced but impeded by the irradiation. A possible cause to this is discussed at the end of the next section.

Similar observations of lower D values as a result of irradiation have been made by Robertson and MacEwan [13] as well as by Frigerio and Gerevini [14] when studying xenon release from UO_2; no correlation between irradiation dose and non-ideal kinetics is reported.

The mechanism discussed above would explain a time-depending diffusion coefficient at constant temperature unless the rare-gas diffu-

*) The calculation was based on the model of Kinchin and Pease

sion proceeds by an interstitial-interstitial mechanism.*) A second possible but not very probable cause deals with the fact that the composition of the investigated material may change during an anneal at constant temperature, leading to a change of the diffusion coefficient. It appears in connection with UO_{2+x} and is discussed in section 3.

We conclude that there is so far little reason to believe that the non-ideal release (Figure 1) can be caused by a process which is equivalent with a time-dependent diffusion coefficient. The practical consequence is that all such curves have to be evaluated from the slope of a F-$\sqrt{t}$-diagram, cf. section 6.

2 TRAPPING AND CONDENSATION IN THE LATTICE

The non-ideal release of the form observed in Figure 1 may be explained by assuming a trapping mechanism. Rare-gas atoms are initially homogeneously distributed in the host lattice and have to diffuse through the lattice in order to reach the surface. If a diffusing atom happens to arrive at an imperfection which acts as a sink for the rare-gas, it does not further take part in the volume diffusion. The atoms present near the surface of the specimen have a higher probability than those in the interior to escape from the crystal before being trapped. After a time several of those atoms which would normally have reached the surface from deeper layers have been trapped and are excluded from diffusion. The investigator observes therefore a decreasing slope of the release curve corresponding to the decreasing number of diffusing atoms. Thermal movements will, however, limit the hold-up time in the traps, so that the trapped atoms can be released to the host lattice; these atoms are free to diffuse to the surface of the specimen unless they are trapped again. The overall gas release as seen by the investigator will be similar to the one shown in Figure 1.

Greenwood, Foreman and Rimmer [15] have pointed out that vacancies and dislocations may play an important role in the creation of sinks for the diffusing rare-gas atoms. Their work was initiated in order to explain

---

*) This mechanism will have support from the argument at the end of section 2

bubble formation during irradiation, but the presented mechanism is applicable also to problems in PAD work.

If two rare-gas atoms meet in the lattice, they are able to combine to a pair linked together with the aid of the everywhere existing vacancies [16]. Pairs of rare-gas atoms with a shared vacancy could be formed during a PAD anneal, and the created complex has a diffusion coefficient much lower than that of a single atom. According to this picture the initial burst observed is in fact due to volume diffusion of single atoms.

The creation of complexes according to

$$2\ M + \text{vac.} \rightleftharpoons [M - \text{vac.} - M]$$

could be the first step in the formation of bubbles. However, the random encounter of two rare-gas atoms is very unlikely under normal PAD conditions. By definition, the encounter probability per unit length is equal to the macroscopic cross section $\Sigma = N\sigma$, where N is the number of rare-gas atoms per cm^3, and σ can be estimated as the geometrical cross section of the nearest region surrounding the rare-gas atom. Assuming the radius of this region equal to about 10^{-7} cm, i.e. a few atomic distances, the mean free path $\lambda = 1/\Sigma$ between encounters is of the order of 1 cm at a concentration N of 10^{14} cm^{-3}. Thus, the random encounter of rare-gas atoms in the interior of the specimen is completely unimportant, lest the concentration is considerable higher than 10^{14} cm^{-3}. For samples with grain size dimensions much less than 1 cm this concentration has, of course, to be correspondingly higher.

As an example, if the diameter of the specimen is d = 0.5 cm, N = 10^{16} cm^{-3}, and arbitrarily assuming that by every random encounter two rare-gas atoms are immobilized, the over-all fraction ($\approx \lambda/d$) of atoms reaching the surface as single atoms during the annealing process would be of the order of one per cent. An initial burst of activity could thus be expected from pair formation due to direct encounters.

However, it seems much more probable that the nucleation takes place at defects which are always present in considerable concentration,

e.g. dislocation lines,*) and that this process is by far the most dominating one even at very high concentrations when random encounters may play a certain role. Electron microscope observations by Bierlein et al. [17] support this assumption. These authors investigated uranium samples with a maximum burn-up of 20 per cent. After irradiation at temperatures lower than 250°C small bubbles of about 10^{-6} cm diameter were observed with a density of 10^{10} cm^{-2}. This is the same order of magnitude as can be expected for the density of dislocation lines in this kind of material [18]. When irradiated a higher temperatures or annealed after irradiation, the specimens contained a smaller number of larger bubbles as a result of bubble growth from the primary ones.

The immobilization of diffusing gas in forming gas bubbles in UO_2 during PAD experiments has been shown by Stevens [19]. UO_2 was irradiated and then heated for an hour at 1600°C. The specimen was afterwards crushed and the released xenon was measured as a function of the crushing time. The crushing operation was repeated on a simultaneously irradiated blank specimen, which had not been heated in order to observe how much gas was released when the body was crushed to fine particles. The heat treated specimen exhibited a much larger release, which must have been caused by diffusion of rare-gas into closed pores during the heat treatment. Thus, an additional amount of gas is liberated when the closed pores are cut during the crushing operation.

In-pile investigations performed by Carrol [20-22] also reveal that regions exist in the UO_2 body, in which the rare-gas is collected and trapped for weeks. A sudden increase of the steady state release rate was observed when cooling the specimen; the ratio of Xe-133 : Xe-135 changed thereby from 5.9 to 22. This ratio is theoretically 4.6 at steady rate and a higher ratio can be observed only if the xenon has been excluded from the lattice of fissionable material, allowing the isotope ratio to change as a result of the more rapid decay of Xe-135. The cooling burst was attributed to a phase-transformation

*) The effect may also be thought of as indirect, due to impurity atoms connected with them.

of the UO_2 when the temperature was lowered.[1] This transformation causes gas atoms to be released after being trapped for longer times as a second phase in the specimen.

Hurst [23] has treated the case of rare-gas diffusion theoretically, taking into account trapping and return from the traps to the lattice. The reader is referred to this work for details. A diffusing atom has a certain probability per unit length to be trapped, and a certain probability per unit time to leave the trap again. The resulting gas release curve shows the typical initial burst, and the diffusion coefficient of the rare-gas has, of course, as in the analogous case of pair formation to be determinated from the slope of the curve at origin (slope of the burst). The general form of the curve may give information on the diffusion length before being trapped and the mean life-time in a trap.

A trapping mechanism different from the one discussed above may explain the observations made in the experiments with CaF_2/Ar [9, 12] already mentioned in section 1. The basic assumption is that the argon atoms are diffusing as interstitials and that the diffusion by a vacancy-mechanism proceeds at a negligable rate if the temperature is high enough.[2]

---

1) When the temperature is suddenly increased in a DAD experiment the diffusion release rate does not simply grow to the steady state level corresponding to the higher temperature, but reaches a maximum above this level before it finally drops to the equilibrium value like a critically damped oscillation. This is seen from the relation for the current $j = -D \cdot \text{grad } c$, considering that the gradient does not change instantaneously to the new value while the diffusion coefficient does. On lowering the temperature a corresponding oscillation is obtained but in the opposite direction ("negative burst"). This kind of burst which is typical for the DAD method and not characteristic for non-ideal release, should not be confounded with the enhanced release rate on lowering the temperature found by Carrol.

2) Measurements which are now being performed at this laboratory on doped CaF_2 seem to bear out this assumption.

The observed decrease of the diffusion with increasing neutron exposure can then be a result of trapping *during* irradiation, since the probability that an argon atom is trapped by a neighbor vacancy increases with increasing neutron dose. It is postulated that after intense damage all argon atoms are trapped in vacancies but for a small portion which is free to diffuse as interstitials and is responsible for the release observed. Each time the temperature is raised in course of the experiment, the thermal movement permits an ever larger portion of the argon atoms to escape from the traps and diffuse as interstitials. The Arrhenius plot for such a release should *not* be a straight line but should asymptotically approach the straight line valid for low radiation damage. This is in effect what has been experimentally observed [12]. A closer examination also shows that this kind of trapping mechanism causes only an unimportant deviation from ideal diffusion kinetics, again in agreement with the performed experiments. Of course, the above reasoning applies also in the case that the traps be physically equivalent to more complicated defects than single vacancies.

3 SURFACE EFFECTS

There are several indications that surface effects may cause an initial burst of release. Consider a surface layer in which the diffusion is considerably faster than in the bulk of the crystal. The initially homogeneously distributed gas atoms will then behave differently on annealing. The surface layer will be rapidly emptied of its gas content producing an activity burst, whereas the subsequent release will be controlled by the kinetics of slow volume diffusion from the bulk, regarding the diffusing atoms as free when reaching the surface layer. As the slow process can be regarded as wholly independent of the rapid one, this corresponds to the model treated in section 6.3. Uranium dioxide can be chosen as illustration. This material is extremely sensitive to oxidation, and it is known from investigations by Lindner and Matzke [24] that the release rate of rare-gases increases rapidly with increasing oxygen content in UO_{2+x}. An oxidized surface will therfore cause an initial burst in this material according to the mechanism described above.

Another possible explanation of the burst could be given if it is assumed that a diffusion transport of excess oxygen takes place from the oxidized surface into the bulk on annealing. In the outer layer the diffusion coefficient will sink as does the oxygen content, and the release rate is observed to decrease. For this mechanism the model of time-dependent diffusion coefficient described in section 1 would apply.

However, it is likely that the release mechanism in UO_2 is more complicated due to its phase instability. Contrary to what has been believed it is not possible to freeze in and obtain a single UO_{2+x} phase at room temperature. This has been studied with electron microscopy by Blank [33]. He found that a disproportionation into UO_2 and U_4O_9 has taken place in all cases where x is greater than 0.0007; the limit of solubility of oxygen in UO_2 lies somewhere between 0.0001 and 0.0007. The U_4O_9 phase was found to be present as coherent precipitations, e.g. minute domains with the coherence of the host lattice preserved. On annealing these precipitations become incoherent or

are eventually dissolved at high enough temperatures. This may cause the release of rare-gases to be higher with higher values of x.

An interesting experiment was performed by Stevens, MacEwan and Ross [25] in order to show that an oxidized surface causes an enhanced release rate. They oxidized the surface of UO_2 powder and used this material in PAD experiments. The release curves showed pronounced bursts, while a specimen which was reduced before the anneal did not show an initial burst.

Similarly, experiments performed on UO_2 single crystals by Barnes et al. [11] resulted in a high initial release rate, which was thought to be a result of oxidation of the surface of the specimen. One of the specimens had a thin oxide surface layer as indicated by electron micrographs and showed a very high initial release rate.

Berry et al. [26] kept UO_2 pellets in humid air for 6 to 12 hours at $20^{o}C$ and observed in subsequent PAD experiments that the release was 10 to 20 times higher than normal. Furthermore, an increase in temperature caused a burst, which was the larger the more rapid the temperature was changed.

An activity burst may have such a trivial reason as a rough surface. For the atoms situated in the most superficial layers of the body the real microscopic surface (which is much larger than the macroscopic one) is of significance in controlling the rate of diffusion. Atoms reaching the surface in a later stage of the experiment have diffused a comparatively longer distance from the inside of the crystal and will not be influenced by the fine-structure of the surface. The slope of the release curve may in the initial stage appear larger than corresponding to the macroscopically measured surface. This effect should be more pronounced for mechanically crushed material than for a large single crystal and should disappear or at least be markedly affected by tempering before irradiation. The fact that the microscopic surface is important for the nearest atoms only is illustrated in Figure 3, which is a simplified picture of a rough surface. As the diffusion follows the concentration gradient, which is in every point perpendicular to the iso-concentration lines, the effec-

tive surface for atoms situated in the bulk will be smaller than the microscopic one and ultimately equal to the geometrical one.

A surface effect, possibly of this kind, which caused an initial burst of activity was found by Kalbitzer when investigating the release of Ar-39 from KC1 [27]. Single crystal material was crushed, sifted into fractions, and irradiated. The subsequent PAD release curves at 107°C showed bursts which were more pronounced for small grains than for larger ones. If the powder was annealed at 550°C for some hours prior to the irradiation, then the curves showed an ideal behaviour. The observed anomalies are apparently due to surface phenomena, the nature of which is not quite clear but may be caused surface diffusion or by the presence of a rough surface as described above.

A body which is subject to irradiation by heavy nuclei exhibits radiation damage of various kinds. The creation of "craters", i.e. highly disturbed lattice regions when introducing Rn and Tn in a crystal by recoil was postulated by Flügge and Zimen [28] on basis of experimental evidence. The disturbed regions were thought to have a connection with the surface so that the rare-gas atoms can easily leave the crystal upon heating; the existence of the craters was discussed in detail by Zimen [29].

Strong radiation effects must also result if fission products are recoiled into the surface of a specimen. Morrison et al. [30] in this way introduced Xe-133 into single crystal alumina and studied the release of xenon during PAD heating. A pronounced initial burst was registered, and when raising the temperature a new burst was observed. This behaviour is possibly connected with the healing out of the defects introduced by the heavy fission fragments, and a step-wise healing process connected with several different activation energies is probable.

Similar effects arise when introducing rare-gas in metals by ion-bombardment. Norton and Tucker [31] have studied the release of krypton introduced in this way into the surface of uranium foils. A subsequent PAD anneal resulted in a release rate of krypton which is much higher than in those experiments where the uranium has undergone fission and therefore the krypton is homogeneously distributed in the specimen.

A special kind of disturbed region is present in reactor fuel material in form of fission spikes [32] which are created all over the irradiated specimen. The spikes should at least partly heal out during an annealing process; a rare-gas atom located in a spike may easily be released if the spike is connected with the surface of the specimen [28] [22]. Thus, a burst of rare-gas atoms can be expected originating from a surface layer with a depth corresponding to the diameter of a spike. Being a surface effect, the burst should be more pronounced the larger the surface of the specimen, notably important for powders and pressed compacts. For uranium Brinkmann gives theoretically calculated values of spike diameters in the order of 10^{-6} cm. This is the same order of magnitude as the surface layer depth, which can be calculated with data (height of burst and surface of the specimen) taken from an experiment performed by Barnes on UO_2 single crystals of integrated thermal neutron exposure nvt = 5.4×10^{17} cm^{-2} [11, Tables 3-4 Figure 7]*. On the other hand, Felix [34] observed a burst from UO_2 single crystal spheres with nvt = 1.5×10^{17} cm^{-2}, which was about ten times larger than what would have been expected from this picture; it would correspond to a spike diameter of about 10^{-5} cm.

The surface effects described above due to radiation damage have one important property in common. They cause rare-gases to be released by a process, which should not be identified with diffusion but rather with recovery of the lattice. This fact may have consequences on the interpretation of gas release data, particularly when the diffusing atoms are fission fragments or when they are introduced in the lattice by a recoil process. If a powder with very small grain size (e.g. of the same order as the recoil range) is used, the total amount of rare-gas may be released mainly as a result of lattice recovery. When so, it is to be expected that the activation energy of the studied release process is the same or nearly the same for different rare-gases. Such results were indeed reported [35] and can probably not be interpreted as being due to diffusion.

---

*$d \cdot S/V = F_B = 5.8 \times 10^{-5}$, (S/V is the surface to volume ratio of the single crystal), from which the spike diameter is calculated to be $d = 2 \times 10^{-6}$ cm.

4 POWDERS AND POLYCRISTALLINE MATERIALS

4.1 Influence of grain size

When the grain size becomes small the recoil losses of rare-gases become important. The relationship

$$\varepsilon_R = \frac{3}{4}\left(\frac{R}{r}\right) - \frac{1}{16}\left(\frac{R}{r}\right)^3 \qquad (4\text{-}1)$$

was derived by Flügge and Zimen [28] and gives the fraction leaving by recoil (ε_R) as a function of the recoil range (R) and the radius of the particles (r). Taking UO_2 powder with a particle size of 50 μ as an example and estimating the recoil range to R = 6 μ, about 18 per cent of the fission fragments should be lost by recoil. Thus, when irradiating such a powder in an evacuated vial, up to 18 per cent of the xenon atoms will enter neighbor particles by recoil. As was described in section 3, Morrison et al. [30] found that recoil-induced xenon was released from alumina in form of bursts; only part of the xenon was released at a certain temperature, so that the temperature had always to be increased to cause further release.

A similar behaviour can be expected when investigating UO_2 powder. Experiments were performed at this laboratory by Felix [34] who found bursts of 2-3 per cent of the total xenon content at 1000°C with the 50 μ powder referred to above. Another portion of the same material was mixed with sodium carbonate powder (volume ratio 1 : 20) before irradiation in order to separate the UO_2 grains from each other with a distance larger than the recoil range and thus preventing the xenon atoms to penetrate into neighboring UO_2 grains. After having separated it from the sodium carbonate, the UO_2 was annealed, and this time no burst was observed. The xenon content of the carbonate varied from 13 to 18 per cent.

4.2 Influence of grain size distribution

Consider a PAD-experiment performed with a powder consisting of spherical single crystals. Pure volume diffusion is assumed to govern the release of rare-gas. It is evident that a burst of activity may be observed when investigating such a powder, if it contains a high percentage

of small sized particles. An extreme case is shown in Figure 4, illustrating the kinetics for a powder mixture made up of only two fractions: 50 w/o of the mixture has particles of a radius r = a, the rest has a radius r = 10 a. Each fraction releases gas according to Figure 4, and the investigator observes the compositive curve, which exhibits an initial burst of activity.

A powder mixture has normally quite another particle size distribution, and one may choose a typical UO_2 powder [37, 38] as an example, with particle sizes ranging from 10 μ to 60 μ. Figure 5 shows the release curve resulting from each fraction, cf. [38]. The sum of these curves is the observed one and is drawn in Figure 6 together with the curves which had resulted from only a 30 μ, and a 40 μ -fraction respectively. The 30 μ size is apparently representative for the mixture and approximates the true curve remarkably well up to F = 0,5, in spite of the complex behaviour of the mixture.

The ideal release pattern from UO_2 powder with a grain size distribution similar to the one used by Matzke and Lindner [39] is shown in the Figures 7 and 8. The compositive curve approximates a 0,11 μ -powder and does not deviate very much from the one resulting from a powder consisting of only 0.10 μ -particles (Figure 8). It is evident that the observed release does not give any indications of the underlying, more complex release if a powder with a normal particle size distribution is used, nor is a burst to be expected.

4.3 Pore desorption and grain boundary diffusion

Radioactive gas which has collected in open pores and microcracks of the specimen will of course be easily released upon heating and may be observed as a burst.

Similarly, grain boundaries permit a higher diffusion rate than does the lattice [40, 41], and the gas atoms located in grain boundaries are likely to leave the specimen upon heating in form of a burst.

Some experiments performed at this laboratory on uranium metal indicates the existence of gas release due to grain boundary diffusion [42].

An irradiated uranium specimen was heated in vacuum above its melting point, and after cooling a normal, multi temperature PAD anneal was performed. During melting only part of the fission gases is released [43], and during solidification a large part of the remaining gas is thought to enter the grain boundaries. The release was found to be some orders of magnitude greater than that for a blank specimen (Figure 9).

4.4 Sintering and grain growth

Sintering and grain growth are related phenomena and may occur in a polycrystalline material during a PAD experiment, though the influence upon the rare-gas release seems to be a matter of discussion.

Auskern [44] favors the opinion that the release rate decreases as a result of sintering because of the increase in grain size. The grain growth is a well known phenomenon in reactor fuel materials. MacEwan [45-47] has investigated UO_2 and found that the increase of the mean grain diameter, d, after annealing for t hours at $T^{o}K$ is given by

$$d^2 - d_o^2 = k_o \times t^{0.8} \exp(-87{,}000/RT)$$

The effect of this surface decrease should of course be a lowering of the release rate.

However, sintering and grain growth imply that part of the lattice constituents drastically change their places. The kinetics of sintering of NaCl has been studied [48], whereby the interfacial growth between spheres of NaCl was observed at 700-800^{o}C. Sintering seems to occur by an evaporation-condensation mechanism with the rate-controlling step assumed to be the diffusion of NaCl-vapor through a thin boundary layer adjacent to the condensating surface.

A similar mechanism seems to govern grain growth in sintered UO_2 according to Canadian investigations [45-47, 49-50]. The oxide vaporizes at the hotter surface of a pore and condenses on the cooler one, permitting the pores to migrate to the center of the pellet where the temperature is highest. The grain boundaries continue to move and certain grains grow at the expense of others, though the changes become slower with time at constant temperature. In view of these findings one can expect those rare-

gas atoms which are located in the regions subject to sintering and grain growth to change their position in the lattice. A part of the fission products are dumped into grain boundaries within the specimen and may thus be released without being involved in volume diffusion through an undisturbed lattice. The result should be an increase of the release rate; it is therefore questionable whether sintering and grain growth lead to an increase or a decrease of the release rate. Experimental evidence has been obtained at this laboratory indicating that sintering and grain growth may result not only in an increase of the release rate but also in creating an initial burst [51]. Ar-41 was introduced in pressed pellets of KF by an (n, p)-reaction, and the influence of pre-heating upon the gas release was studied. If the green pellet was used without tempering a pronounced burst was observed (Figure 10) and a visual grain growth had occurred. After pre-heating at 800°C for one hour, the release curve showed a small burst only and was similar to the release of argon in single crystal KF (Figure 10). The specimen had been subject to far-reaching grain growth during the pre-heating.

Further, experiments with powdered UC [42] showed release curves not only with an initial burst, but also a second smaller burst at about 1500°C (Figure 11). This is thought to be due to a beginning sintering, as the powder particles clearly adhered to each other, but not to the tantalum container material, after heat treatment at about 1700°C.

There does not seem to be any physical-mathematical picture which can be used for the evaluation of PAD release curves if grain growth and sintering occur. Information of technical importance may result from such experiments but it would be futile to expect diffusion coefficients of acceptabel accuracy.

DAD loops could be used to study these effects and to determine diffusion coefficients from the steady state release after sintering, phase transformations or chemical changes (cf. next section) have occured.

5 OTHER CAUSES TO NON-IDEAL RELEASE

5.1 Phase transformations during the annealing process

It has been proved by Scott and Buddery [52] that phase changes in uranium metal enhance the release rate during a PAD experiment. Significant release of krypton occurs which is apparently associated with the $\alpha \rightarrow ß$ transformation. The peaks in the release rate are of short duration ard correspond to a release of the order of 0,1 % every time the transition temperature is reached.

The burst of activity found in DAD work on UO_{2+x} when cooling is thought to be due to the increased mobility during a phase change of the specimen [20-22]. Furthermore, Carrol has shown that the gas released in a cooling burst has for a longer period of time been trapped within the specimen [20-22], cf. section 2.

These cooling bursts have been thoroughly investigated in PAD experiment by Rothwell [53, 54]. The uranium dioxide loses oxygen above 1800°C and becomes substoichiometrical (UO_{2-y}); on cooling UO_{2-y} transform into UO_2 and uranium metal [53], whereby the mobility of the atoms in the lattice is enhanced. The release during this transformation is considerable and may amount to a third of the total activity [54].

According to recent observations [45, 53, 55] pure uranium dioxide may precipitate uranium metal as a second phase on annealing at high temperatures in atmospheres of low oxygen pressure. These metallic inclusions are only a few microns in diameter and may be detected metallographically. Arc-melted UO_2 contains uranium in grain boundaries and uranium is also uniformly dispersed throughout the grains. At 1130°C the uranium located in the grain boundaries melts and liberates its contents of fission gases.

The presence of metallic uranium in arc-fused pieces of single crystal UO_2 was suspected by investigators at the Battelle Memorial Institute [11], and was thought to cause a sharp but small burst of the release rate during a PAD anneal.

5.2 Chemical reaction of the specimen during the PAD annealing process

Gas releases as low as 10^{-3} % are often observed during a PAD experiment. Such small amounts of gas originate from so thin a surface layer that corrosion to the same depth is normally not detected. One has then to take gas release due to corrosion into consideration.

It is a well known phenomenon from metallurgy that such a surface oxidation layer may be porous and permeable for gases. Therefore the release will be influenced by the corrosion, which cannot however be discovered or separated from the diffusion because a $\sqrt{t}$-law may govern the kinetics of both phenomena. If the rare-gas content is immediately set free upon formation of a spongy surface layer, the diffusion kinetics will be unimportant for the release. In this case the investigator will observe the kinetics of corrosion only. Extreme care has to be taken when working with materials which are suspected to react with the ambiant atmosphere or with the container materials.

Even if these conditions are fulfilled one may have trouble in keeping the chemical composition of the specimen unchanged. Uranium oxide with a composition between $UO_{2,0}$ and $UO_{2,2}$ should have to be annealed in an atmosphere containing oxygen of a partial pressure, which is dependent upon the temperature, because the partial pressure of oxygen has to match the equilibrium pressure at that temperature; c.f. the experiments of Stevens et al. cited in section 3 [25].

Uranium metal is a strong getter for oxygen and nitrogen, and it is extremely difficult to eliminate a surface reaction when heating the metal. Oxidation of uranium is known to be accompanied by release of fission gas [43, 56], and oxidation of a surface layer only some Ångström thick may account for the observed release [57, 58].

The initial burst registered when PAD heating a uranium specimen [42] may well be caused by oxidation, Figure 12. Uranium metal may however react also with container materials such as quartz [42, 59], and the use of tantalum containers during the heat treatment seems to be necessary [60]. A good check is the use of an electropolished, bright specimen, the surface of which would be tarnished by a very thin, possibly monomolecular layer,

if oxidation has occured during the run.

Uranium monocarbide is also chemically reactive, and great care has to be taken in order to choose a suitable method of investigation [7]. It was found in this laboratory [42] that the release of xenon from UC was affected by the material, with which the specimen was in contact during the PAD heating. A solid-solid reaction occured between specimen and container, enhancing the diffusion. A pronounced burst was not observed, but the release was many times higher than during an experiment using a chemically indifferent tantalum or tungsten container, Figure 13. Similar observations on UO_2 are reported [26].

5.3 Evaporation of the specimen during the anneal

When working in vacuum systems at high temperatures one almost always observes weight losses of the sample during the experiment. When evaporation has taken place, its influence upon the release kinetics has to be considered. The evaporation losses per unit time ought to be proportional to the surface, which means that the radius diminishes with a constant rate

$$- dr/dt = g, \qquad (5\text{-}1)$$

if for simplicity, we consider a spherical body.

This leads directly to the expression

$$F_e = 3\frac{g}{r}t - 3\frac{g^2}{r^2}t^2 + \frac{g^3}{r^3}t^3 \qquad (5\text{-}2)$$

where F_e denotes the fractional mass loss due to evaporation and r the initial radius of the sphere.

The general behaviour of F_e as a function of the square root of t is shown together with the normal diffusion release F in Figure 14. One can discuss qualitatively the influence of evaporation on the release by use of Figures 14-18 without solving the diffusion equation containing a time-dependent radius due to evaporation losses.

F_e has quite a different kinetics than F, and as it is increasing very slowly (parabolic) for small F_e-values, it could possibly be mistaken for

diffusion at higher F_e values only. If the release were mainly due to evaperation and the diffusion unimportant, the initial parabolic part should clearly expose this.*) If, on the contrary, the initial part is linear indicating pure diffusion, the curve may later deviate from the ideal behaviour as evaporation grows more and more important relative to the diffusion as time goes on. A rapid method to discover such a deviation is described in [10, 12] and some illustrations are given in Figure 15. Each value of the function φ^2 is formed from the corresponding value of F^2 belonging to the same time. In the case of ideal diffusion, φ^2 should be identical with the extrapolated tangent of the F^2-t-curve at the origin. In the case of evaporation φ^2 should not be a straight line but should bend upwards. This is seen to occur in Figure 15b; therefore the deviation from diffusion release could possibly be explained as caused by the simultaneous evaporation.

Experiments from this laboratory on argon diffusion in calcium fluoride evaluated with this method show that the influence of evaporation may not be as great as might be expected in the first instance. Although evaporation is observed in the high temperature stages of the experiments indicated by Figure 15a and c, the release seems to be perfectly ideal. That this is so might be qualitatively explained in the following way. Evaporation can increase the release only by accelerating the transport of rare gases in the utmost surface layer. However, the concentration of rare gases in these layers is high only in the very beginning of an anneal, when the evaporation is negligable relative to diffusion; then it rapidly falls. Later, when the evaporation has grown important, the gas atoms arriving at the surface have already travelled from the inside of the crystal a distance large enough to make the surface transport unimportant for the kinetics.

The surprising result, that in the case of calcium fluoride the simultaneous evaporation of the crystal during the diffusion anneal does not disturb the release kinetics to any remarkable extent may or may not be true for crystals of other materials under similar conditions. In order to be able to predict this, the evaporation effects were estimated and compared for CaF_2, KCl, UO_2, and ThO_2 in the following manner.

---

*) Provided this part of the curve is not obscured by a burst.

Consider the concentration profile in a sphere of radius r at the time t, according to Figure 16. This profile is approximated with the dotted square edge profile through the inflexion point, which is equivalent to saying, that the boundary of uniform concentration has moved the distance $\sqrt{Dt}$, the diffusion depth (for the following estimation the factor $\sqrt{2}$ was left out of account). At the same time the radius of the sphere has diminished by the amount gt due to evaporation of the surface. As long as gt is small compared with $\sqrt{Dt}$, it is to be expected, that the diffusion is not appreciably influenced by the evaporation.

The magnitude of g was determined experimentally according to equation (5-1) for different temperatures; the results are shown in Figure 18. The values for ThO_2 are preliminary values, based on early data of Felix [34]; however, only the order of magnitude is of interest in this connection. According to Figure 17, at the beginning of the anneal, the diffusion front moves faster than the evaporation front, but it is ultimately reached by the latter at the point where $r_d = r_e$. (If this point has a physical significance or not - even at the validity of the above approximation - depends on the actual values of g and D, cf. below.) For comparison between different crystal materials the quantity

$$t_o = \frac{D}{4g^2}$$

was calculated. For $t<t_o$ the evaporation front moves behind and always slower than the diffusion front (at t_o the two fronts are separated by the largest distance), and the evaporation should have no noticeable influence on the diffusion kinetics.

As an example consider calcium fluoride at 1150°C and pressure of 1-2 torr in the gas phase with $D = 1.5 \times 10^{-6}$ cm^2/s and $g = 8 \times 10^{-5}$ cm/min.

Then $$t_o = \frac{60 \times 1,5 \times 10^{-6}}{4 \times 64 \times 10^{-10}} \text{ min} = 60 \text{ hours}$$

The approximation according to Figure 16 is valid, provided that

$$\sqrt{Dt} \ll L,$$

that is

$$t \ll 1/D = 10^6/1.5 \text{ seconds} = 180 \text{ hours}$$

if the length L of the crystal is of the order of 1 cm. As the duration of an experiment at 1150°C is of the order of some hours, the validity is fullfilled during the whole annealing process. It is not so amazing therefore in view of the high value of t_o, that the kinetics appear to be ideal. For 1300°C the time t_o is calculated to 1.5 hours, which means that a perturbation of the kinetics due to evaporation cannot be excluded at that temperature, at least not towards the end of the experiment. This does not, however, prevent the accurate determination of D, cf. Figure 15b.

The results of the estimation for different crystals are summarized in table 5-1, which clearly indicates that evaporation raises no problems in connection with CaF_2, KCl, and ThO_2 crystals but becomes very critical in the case of UO_2. It is experimentally observed [34] that the $F(\sqrt{t})$ plot is linear up to much higher F values than theoretically expected. This is probably due to the fact that the release is built up of both evaporation and diffusion. A clear consequence of this is a seemingly abnormal high activation energy. The activation energies for xenon diffusion in UO_2 reported in the last years are also extremely high; they show a strong tendency to grow even higher.

A single evaporation measurement seems to be a necessary step in planning an investigation of rare gas diffusion in any kind of material.

Table 5-1: Influence of evaporation on the diffusion kinetics

System	Temp. °C	$D/4\ g^2$	$1/D$
CaF_2/Ar (1-2 torr)	1150 1250 1300	60 h 5 h 1.5 h	180 h 40 h 20 h
KCl/Ar (10^{-3} torr)	500 600 700	8 h 20 h 40 h	1000 h 30 h 2 h
UO_2/Kr (10^{-3} - 10^{-2} torr)	1500 1600 1700	10 h 20 m 1 m	10^{11} h 10^{10} h 10^{9} h
UO_2/Xe (10^{-3} -10^{-2} torr)	1500 1600 1700	20 m 1 m 2 s	10^{9} h 10^{8} h 10^{8} h
ThO_2/Kr (10^{-3} torr)	1700 1800	10^{4} h 50 h	10^{8} h 10^{8} h

5.4 Changed concentration profile due to flux depression

The diffusion equation valid for PAD experiments is always solved under the assumption that the concentration of rare-gas atoms is constant throughout the specimen at the time t = 0

Consider a sample of pure uranium metal with dimensions of the order of 1 cm. The rare-gas concentration in the body after irradiation will vary roughly as $e^{-\Sigma x}$, where x is the distance from the surface and Σ is the product of the fission cross section for U-235 and the enrichment α. Thus the gas concentration in the center of the specimen is roughly $e^{\alpha . 23,6 . 0,5}$ less than at the surface. For pure U-235, a material with no practical importance, this factor is about 10^6, which should lead to a pronounced initial burst during a PAD experiment. The factor rapidly decreases with decreasing enrichment, being about 10 for α = 20 % and about 3 for α = 10 %. Thus, the self-absorption of slow neutrons by the sample during irradiation can be excluded as the possible cause of initial bursts described in the literature, because no measurements were made with heavily enriched materials.

6 NOTES ON THE EVALUTION OF NON-IDEAL RELEASE CURVES

6.1 Introduction

The evaluation of release curves exhibiting an ideal diffusion pattern is covered by Lagerwall and Zimen [10] and is not discussed here. In contrast to the quantitative treatment in [10] this section is only intended to stress the general principles and difficulties.

The published data on diffusion of fission rare gases in reactor materials are strikingly inconsistent with each other. One of the reasons to this may be that several investigators misinterpret the results because their methods of evaluation are inadequate, being valid only for the case of undisturbed volume diffusion. It is here pointed out why these methods often fail and how the correct diffusion coefficients may be obtained from experimental data.

6.2 Time-dependent diffusion coefficient

The solution of the diffusion equation

$$\frac{\partial c}{\partial t} = D \nabla^2 c \qquad D = \text{const.} \qquad (6\text{-}1)$$

has been given for PAD problems by Inthoff and Zimen [2], who express the kinetics in the approximation

$$F^2 = \frac{4}{\pi} (S/V)^2 \, Dt \qquad (6\text{-}2)$$

where S/V = surface-to-volume ratio

Equation (6-2) is valid for pure volume diffusion at a constant temperature as long as $F \lesssim 0{,}25$.

Assuming a time-dependent diffusion coefficient, e.g. in the case that the temperature is changed during the annealing process, equation (6-1) may be rewritten in the form, cf. [36]

$$\frac{\partial c}{\partial \Theta} \cdot \frac{\partial \Theta}{\partial t} = D(t) \cdot \nabla^2 c \qquad (6\text{-}3)$$

and the new variable Θ so determined that

$$\frac{\partial \Theta}{\partial t} = D(t) \qquad (6-4)$$

giving

$$\frac{\partial c}{\partial \Theta} = \nabla^2 c. \qquad (6-5)$$

Equation (6-5) is identical in form with (6-1) assuming D be equal to one; consequently, its solution corresponding to (6-2) is

$$F^2 = \frac{4}{\pi} \left(\frac{S}{V}\right)^2 \Theta \qquad (6-6)$$

Therefore a plot F^2 vs t has a slope

$$\frac{dF^2}{dt} = \frac{4}{\pi} \left(\frac{S}{V}\right)^2 \frac{\partial \Theta}{\partial t} = \frac{4}{\pi} \left(\frac{S}{V}\right)^2 \cdot D(t),$$

that means, the curve has a slope which in every point is proportional to D , no matter how D is changing. Consider for instance the case that the temperature is raised twice during the annealing process, corresponding to the curve in Figure 19. Θ is obtained from (6-4) to be

$$\Theta(t) = \int_0^t D(t')\, dt'. \qquad (6-8)$$

Thus, in this case

$$\Theta(t) = \int_0^t D_1\, dt' + \int_{t_1}^{t_2} D_2\, dt' + \int_{t_2}^{t} D_3\, dt' = D_1 t_1 + D_2(t_2 - t_1) + D_3(t - t_2). \qquad (6-9)$$

This means that the $F^2(t)$-plot consists of three linear parts, corresponding to the three constant diffusion coefficients D_1, D_2 and D_3 (Figure 19). In order to see what shape an $F(\sqrt{t})$-plot will have for the same experiment, we first note that the diffusion equation (6-1) may be written

$$\frac{\partial c}{\partial (Dt)} = \nabla^2 c \qquad (6-10)$$

from which it is clear that D and t can never appear seperated in the solution, but always in the combination Dt. Consequently, it does not matter for the concentration profile of gas atoms in the specimen, whether a certain fractional release F has been reached on annealing at the temperature T during the time t or at the temperature T' during the time t', provided that the product Dt is the same in both cases. This means that when the temperature is changed from T_1 to T_2 at the point P in Figure 20, the $F^2(t)$-plot proceeds exactly in the same way as if the anneal had been performed all the time at the temperature T_2 with the beginning of the anneal displyced the amount δ. In an $F(\sqrt{t})$-plot the part a is of course linear, the part b not, because the latter does not start from the origin; b has the equation

$$F^2 = \alpha^2 (t - \delta). \qquad (6\text{-}11)$$

In an F, $(\sqrt{t})$ coordinate system it becomes

$$F^2 = \alpha^2 (\xi^2 - \delta) \quad \text{where } \sqrt{t} = \xi \qquad (6\text{-}12)$$

or

$$\frac{\xi^2}{\delta} - \frac{F^2}{\alpha^2 \delta} = 1 \qquad (6\text{-}13)$$

Equation (13) represents a hyperbola with the asymptote

$$\frac{\xi^2}{\delta} - \frac{F^2}{\alpha^2 \delta} = 0 \qquad (6\text{-}14)$$

which means that

$$F = \alpha \xi = \alpha \sqrt{t} \qquad (6\text{-}15)$$

The evaluation should apparently be made from the asymptote of the $F(\sqrt{t})$-curve, which is in practice difficult. Besides, the plot leads to the principal misinterpretation as discussed in section 1, by simulating small bursts at T_2 and T_3 which do not exist, and by enlarging already existing ones. The consequences of plotting F vs $\sqrt{t}$ when the temperature is changed is seen in Figure 21, where the correct asymptotes

have been drawn also. As these curves are unsuitable for evaluation, the $F^2(t)$-plot has to be used in the case of time-dependent diffusion coefficient. Note that the discussion has assumed that no overlapping bursts affect the gas release, cf. section 6.3.

6.3 The case of overlapping processes

Consider an experiment in which the fractional release, F, is accumulated and measured. Suppose that the release due to pure volume diffusion, f, is overlapped by an activity burst from a source which is rapidly exhausted (Figure 22); after a time t_o, the burst contributes with a certain constant value, b, to the activity in the gas phase*). The measured fractional release F is after a certain time (t_o) equal to f + b and has the same slope (α) as f. The diffusion coefficient, which has to be determined from the experiment, is proportional to α^2.

Upon squaring F one gets (for $t > t_o$)

$$F^2 = (f + b)^2 = f^2 + b^2 + 2\,bf = \alpha^2 t + b^2 + 2b\alpha \cdot \sqrt{t} \qquad (6\text{-}16)$$

and the slope of the curve $F^2(t)$ is

$$k(t) = \alpha^2 + 2b\alpha \cdot \frac{1}{2\sqrt{t}} = \alpha^2 + b \cdot \frac{\alpha^2}{f} = \alpha^2 \left(1 + \frac{b}{f}\right). \qquad (6\text{-}17)$$

As can be seen from (6-17) and from Figure 23, this composite slope does not correspond to a straight line, though the deviation normally lies within experimental error. Thus, from the slope of $F^2(t)$ a diffusion coefficient is calculated, which is larger than the real one, affected with a relative error equal to b/f.

If for instance b is about 10 times larger than f, a quite frequent case, a slope about ten times too large is found. On rewritting (6-17) into

$$k = \alpha^2 \frac{F}{b} = \alpha \frac{F}{f} \qquad (6\text{-}18)$$

it is seen that

$$\alpha^2 = k^2 \frac{t}{F^2} \qquad (6\text{-}19)$$

*) The decay is neglected, being unessential for the problem.

As $\varkappa^2$ is proportional to the real diffusion coefficient, a correct value can be arrived at from the three observed quantities K, t , and F^2 in an $F^2(t)$-plot . Nevertheless, this method may be disadvantageous if the measurement is not accurate enough to allow a determination, which point on the $F^2(t)$-plot actually corresponds to a certain k-value. In addition, with this plotting the mere presence of a burst at the initial stage will cause a small "burst" at each subsequent change of the temperature (c.f. Figure 23 and section 6.2), although the diffusion may be perfectly ideal. In this case the $F^2(t)$-plot leads to a misinterpretation of the response to a temperature change. Consequently, whenever a burst occurs, the evaluation has to be made from a plot F vs$\sqrt{t}$.

In many experiments, which are described in the literature in terms of F^2 vs t, not only an initial burst appears, but the temperature is also changed several times. One realizes from the discussion above that the evaluation of diffusion coefficients from the slope of these plots cannot be correct. On the other hand plotting of F ($\sqrt{t}$) would not be suitable either, though in this case the first stage of the anneal is correctly represented (Figure 21). There is no simple straight-forward method of evaluation in this case, unless the release activity is high enough to permit measurement of the release r a t e with an acceptable accuracy. Of course, the rate cannot be influenced by the previous history of the release, e.g. initial bursts, unless the concentration profile is thereby drastically altered,* a fact which is notably advantageous in DAD measurements.

The best thing to do in order to evaluate experiments of this type would probably be to plot a curve as the one drawn in Figure 24. Here F is a function of$\sqrt{t-t_i}$ where t_i is the time at which the temperature is changed. Most important, as in the F ($\sqrt{t}$)-plot the first annealing

---

*In several cases the evaluation of D from an F ($\sqrt{t}$)-plot could perhaps be somewhat improved if it is assumed that a large burst causes a depletion of the outer layers analogous with the effect of recoil losses. The slope after the burst ought then to be doubled before calculating the D-value as long as $b \approx F$, cf. [2].

stage gives directly the correct value of D. The succeeding curve branches are hyperbolas as in the F($\sqrt{t}$)-plots. However, they approach the asymptotes more rapidly, and could not be mistaken for small bursts, being hyperbolas in the conjugate position. As is seen in Figure 25, a second smaller burst at the temperature T_2 may also be detected in this way without affecting the evaluation of D too much, provided that the anneal at each temperature is not performed over too short a time*

6.4 The case of competing processes

This case is thoroughly covered by Hurst in a recent report [23]. Assuming the existence of trapping centres and other sinks for diffusing rare-gas atoms, the initial part of the release curve is of course the significant one for the determination of the diffusion coefficient. Of multitemperature anneals only the first stage will be possible to evaluate.

6.5 Conclusions

From the preceding sections it is clear that whenever bursts appears, one may get doubtful information by performing multi-stage anneals instead of working at a constant temperature. If one has evidence that the cause is not of the type discribed in 6.4 and would prefer multi-temperature anneals from reasons of experimental convenience, the best way of evaluating such an experiment is probably in terms of an F ($\sqrt{t-t_i}$)-plot (Figures 24-25). In this case, each stage should be followed long enough to compensate for the initial non-linearity of the curve.

Another way of performing the evaluation would be to subtract the burst graphically from an F ($\sqrt{t}$)-curve and then plot F^2_{sub} vs t. This is more tedious and probably less accurate because the subtraction errors are in practice large. If several bursts occur during the experiment, this method can therefore not be recommended. The only possibility is then to perform less complicated experiments, e.g. single-temperature

---

* Because the concentration profile actually is changed in a more or less uncontrollable way during a burst, it is an indispensable condition to perform the measurement over long periods of time in such cases, quite independent of the evaluation method used.

anneals. For the sake of convenience, some recommendations regarding evaluation are listed together on the following pages.

6.6 Recommendations for the evaluation of release curves

6.6.1 Release without or with a small burst ($b \ll F$)

Single- and multi-temperature experiments can be properly evaluated over the whole range of F according to [10], (c.f. Figure 15). F ($\sqrt{t}$) can be used for single-temperature anneals but this is not recommended (cf. below a). Recommendations for the evaluation if:

a) specimen reaches temperature slowly. — Evaluate from $F^2(t)$ or $\varphi^2(t)$ as above, not from $F(\sqrt{t})$.

b) single crystal powder material is used. — A rapid and accurate method of evaluation is the following. The grain size distribution can be substituted by a representative mean radius (because otherwise a burst had been observed, c.f. Figure 4). Evaluate according to the corresponding sphere [10]. In the $\varphi^2(t)$ diagram the slope will not be constant but will steadily diminish as F increases from zero to 100 per cent. The mean slope at about F = 50 per cent gives the correct D value. (The same will be true if one plots $\alpha^2 = Dt/r^2$ with the aid of [10] as a function of t and determines D from this slope).

Other methods: a) to construct the correct release curve from the grain size distribution (accurate but tedious), b) to use the expression $F^2 = \frac{4}{\pi}(S/V)^2 Dt$ if the surface S is known from a BET measurement (valid for $F \lesssim 0,3$).

6.6.2 Release with burst ($b \approx F$)

Consequences if the burst is due to:	
a) Trapping or creation of pairs and bubbles	Determine D from the slope at origin in a $F^2(t)$ (or $F(t)$) diagram. This is likely to be difficult in practice, because only a few measuring points can be found by experiment. In that case one has to calculate D from a larger part of the curve using an trial- and error-method [23].
b) Grain boundary diffusion, pore desorption, surface effects (fission spikes, oxidized layer etc.)	Single temperature anneal: plot $F(\sqrt{t})$. Determine D from the slope according to Figure 22; cf. footnote on page 33. Multi-temperature anneal: plot $F(\sqrt{t - t_i})$. This results in hyperbolas; determine D from the slope of the asymptotes.
c) Extreme grain size distribution	As in b). In this case the distribution can be substituted by two representative radii. From the two slopes of the plot according to Figure 4, two values of D are provided, which should of course be similar.
d) Phase transformations	No accurate evaluation method. PAD experiments highly unsuited *)
e) Sintering and grain growth	
f) Chemical reaction of the specimen	

*) These effects are best studied in DAD experiments, measuring the release rate. In this case the evaluation offers no principal difficulties.

ACKNOWLEDGEMENT

The authors should like to thank Dr. F. Felix, Dr. H. Gaus, Dr K. Wagener, and especially Prof. K.E. Zimen for valuable discussions, criticism and contributions. The work was partly promoted by Euratom under contract No 094-62-9RDD.

REFERENCES

[1] Zimen, K.E. Diffusion von Edelgasatomen, die durch Kernreaktion in festen Stoffen gebildet werden (Edelgasdiffusion in Festkörpern 1)
Trans. Chalmers Univ. Technol. (Göteborg)
No. 175 (1956) 1-7

[2] Inthoff, W.
Zimen, K.E. Kinetik der Diffusion radioaktiver Edelgase aus festen Stoffen nach Bestrahlung (Edelgasdiffusion in Festkörpern 2)
Trans. Chalmers Univ. Technol. (Göteborg)
No. 176 (1956) 1-16

[3] Zimen, K.E.
Dahl, L. Die Diffusion von Spaltungs-Xenon aus Uranmetall [(Edelgasdiffusion in Festkörpern 3)]
Z.Naturforschg. 12 a (1957) 167-169

[4] Felix, F. Die Diffusion von Spaltungs-Xenon in Uranoxyd [(Edelgasdiffusion in Festkörpern 4)]
Nukleonik 1 (1958) 66-67

[5] Zimen, K.E. Tabellen für die Auswertung von Messungen der Diffusion radioaktiver Edelgase aus festen Stoffen nach Bestrahlung (Edelgasdiffusion in Festkörpern 5)
HMI-B16, Mai 1961, 28 S.

[6] Gaus, H. Zur Berechnung der Diffusion von radioaktiven Gasen I (Edelgasdiffusion in Festkörpern 6)
Z. Naturforschg. 16 a (1961) 1130-1135

[7] Schmeling, P.
Felix, F. Experimental Methods and Equipment for Diffusion Measurements of Radioactive Rare-Gas Diffusion in Solids (Rare-Gas Diffusion in Solids 7)
HMI-B19, Nov. 1961, 18 S. and
(EUR 111e,1962)

[8] Gaus, H. — Zur Berechnung der Diffusion von radioaktiven Gasen II (Edelgasdiffusion in Festkörpern 8) Z. Naturforschg. 17a (1962) 297-305

[9] Lagerwall, T. — Diffusion of Argon-41 in Calcium Fluoride (Rare-Gas Diffusion in Solids 9) Nukleonik 4 (1962) 158-161

[10] Lagerwall, T. Zimen, K.E. — The Kinetics of Rare-Gas Diffusion in Solids. Tables and Graphs for the Evaluation of Post-Activation Diffusion Experiments (Rare-Gas Diffusion in Solids 10) HMI-B 25, Aug. 1963, 25 p.

[11] Barnes, R.H. et al. — Xenon Diffusion in Single Crystal and Sintered UO_2 BMI-1533, 1961, 40 p.

[12] Lagerwall, T. — to be published

[13] MacEwan, J.R. Robertson, J.A.L. — Private communication, 1962

[14] Frigerio, G. Gerevini, T. — On the Dependence upon Irradiation Exposure of the Apparent Diffusion Rates of Xenon in Uranium Dioxide to be published in J. Nucl. Mat.

[15] Greenwood , G.W. Foreman, A.J.E. Rimmer, D.E. — The Role of Vacancies and Dislocations in the Nucleation and Growth of Gas Bubbles in Irradiated Fissile Material J. Nucl. Mat. 4 (1959) 305-324 AERE-R-2863, 1959

[16] Brinkman, J.A. — Personal communication, 1962

[17] Bierlein, T.K. et al. — Metallographic Observation of Swelling in Uranium HW-63848, 1960, 59 p.

[18] Shockley, W. ed. — Imperfections in Nearly Perfect Crystals Wiley, New York, 1952, p. 48

[19] Stevens, H.W. — as cited by W.B. Lewis [50]

[20] Carrol, R.M. — Continuous Release of Fission Gas from UO_2 During Irradiation Proc. Symp. on Radiation Effects in Refractory Fuel Compounds Amer. Soc. for Testing and Materials, 1961, 110-120

[21] Carrol, R.M. — Fission Gas Release from Uranium Dioxide During Irradiation Nuclear Safety 4 (1962) No. 1, 35-42

[22] Carrol, R.M.
Instantaneous Fission-Gas Release Experiments From Gas-Cooled Reactor Program Quarterly Report for Period Ending Juni 30, 1961 ORNL-3166, 1961

[23] Hurst, D.G.
Diffusion of Fission Gas. Calculated Diffusion from a Sphere Taking into Account Trapping and Return from the Traps AECL-1550, 1962, 40 p.

[24] Lindner, R.
Matzke, H. j.
Diffusion von Xe-133 in Urandioxid verschiedenen Sauerstoffgehaltes Z. Naturforschg. 14a (1959) 582-584

[25] Stevens, W.H.
MacEwan, J.R.
Ross, A.M.
The Diffusion Behaviour of Fission Xenon in Uranium Dioxide from TID-7610 Procs. of First Conf. on Nuclear Reactor Chem. 1960, 7-22

[26] Berry, J.L.
Darras, R.
Chevilliard, H.
Gerevini, T.
Contribution a l'étude de l'échappement des gaz de fission hors de l'oxyde d'uranium fritté irradié J. Nucl. Mat. 8(1963) 102-115

[27] Kalbitzer, S.
Experimente zur Edelgasdiffusion in Alkalihalogenid-Einkristallen Z. Naturforschg. 17a (1962) 1071-1081

[28] Flügge, S.
Zimen, K.E.
Die Bestimmung von Korngrößen und von Diffusionskonstanten aus dem Emaniervermögen. Die Theorie der Emaniermethode Z. Phys. Chem. 42 (1939) 179-220

[29] Zimen, K.E.
Oberflächenbestimmungen und Diffusionsmessungen mittels radioaktiver Edelgase III: Der Vorgang der Emanationsabgabe aus dispersen Systemen. Folgerungen für die Auswertung von EV-Messungen und für die Deutung der Ergebnisse Z. phys. Chem. 192 (1943) 1-55

[30] Morrison, D.L.
Barnes, R.H.
Elleman, T.S.
Sundermann, D.N.
Postirradiation Release of Xenon-133 from Single Crystal Alpha Alumina BMI-1592, 1962, 30 p.

[31] Norton, F.J.
Tucker, C.W.
Krypton Evolution from Metallic Uranium J. Nucl. Mat. 2 (1960) 350-352

[32] Brinkman, J.A.
Fission Damage in Metals NAA-SR-6642, 1962, 50 p.

[33] Blank, H. — Personal communication, 1963

[34] Felix, F. — Personal communication, 1963

[35] Lindner, R. Matzke, Hj. — Diffusion radioaktiver Edelgase in Uranoxyden und Uranmonokarbid Z. Naturforschg. 14a (1959) 1074-1077

[36] Crank, J. — The mathematics of diffusion Oxford (Oxford Univ. Press) 1956

[3 7] Clayton, J.C. Aronson, S. — Some Preparative Methods and Physical Characteristics of Uranium Dioxide Powders J. Chem. Eng. Data 6 (1961) 43-51

[38] Kiessling, R. — Schwedische Untersuchungen über UO_2 als Reaktor-Brennstoff Nukleonik 2 (1960) 198-203

[39] Matzke, H.J. Lindner, R. — Zur Diffusion homogener verteilter Edelgase aus Festkörpern Z. Naturforschg. 16a (1961) 845-849

[40] Bokstein, S.Z. Kishkin, S.T. Moroz, L.M. — Investigation of the Structure of Metals by Radioactive Isotope Methods AEC-tr-4505, 1961, 205 p.

[41] McLean, D. — Grain Boundaries in Metals Oxford Univ. Press, 1957

[42] Schmeling, P. — unpublished results

[43] Hilliard, R.K. — Oxidation of Uranium in Air at High Temperatures HW-58022, 1958, 31 p.

[44] Auskern, A.B. — Further Work on the Diffusion of Kr-85 from UO_2 Powder WAPD-TM-225, 1960, 14 p.

[45] MacEwan, J.R. — Grain Growth in Sintered UO_2 AECL-1184 (CRED-999) 1961, 15 p.

[46] MacEwan, J.R. — Grain Growth in Sintered Uranium Dioxide I. Equiaxed Grain Growth J. Am. Cer. Soc. 45 (1962) 37-41

[47] MacEwan, J.R. Lawson, V.B. — Grain Growth in Sintered Uranium II, Dioxide Columnan Grain Growth J. Am Cer. Soc. 45 (1962) 42-46

[48] Moser, J.B.
Whitmore, D. H.
Kinetics of Sintering of Sodium Chloride in the Presence of an Inert Gas
J. appl. Phys. 31 (1960) 488-493

[49] Lawson, V.B.
MacEwan, J.R.
Thermal Simulation Experiments with UO_2 Fuel Rod Assembly
AECL-994 (CRFD-915) 1960, 30 p.

[50] Lewis, W.B.
Behaviour of Fission Gases in UO_2 Fuel
AECL-1402 (DL-45) 1961, 36 p.

[51] Mundt, H.
Unpublished results
HMI, 1961

[52] Scott, K.T.
Buddery, J.H
The Release of Krypton 85 from Irradiated Uranium on Thermal Cycling through the Phase Change
J. Nucl. Mat. 5 (1962) 94-100

[53] Rothwell, E.
High Temperatures Substoichoimetry in Uranium Dioxide
J Nucl. Mat. 5 (1962) 229-236

[54] Rothwell, E.
The Release of Krypton 85 from Irradiated Uranium Dioxide on Post-Irradiation Annealing
J. Nucl. Mat. 5 (1962) 241-249
AERE-R-3672, 1961

[55] Colombo, R.
Frigerio, G.
On the Occurrence of Uranium Metal Particles in Fused UO_2
J. Nucl. Mat 5 (1962) 259-261

[56] Parker, G.W.
Creek, G.E.
Martin, W.J.
Fission Product Release from UO_2 by High Temperature Diffusion and Melting in Helium and Air
CF-60-12-14, 1961, 51 p.

[57] Gray, D.L.
Release of Inert Gas from Irradiated Uranium (A Review of the Literature)
HW-62639, 1960, 21 p.

[58] Rothman, S.J.
Diffusion in Uranium, its Alloys and Compounds
ANL-5700 (Pt. C) 1961, 56 p.

[59] Müller, N.
Untersuchungen über die Diffusion in den Systemen Uran-Zirkon und Uran-Nickel
Z. Metallkunde 50 (1959) 652-660

(60] Johnston, W.V.
Personal communication, 1962

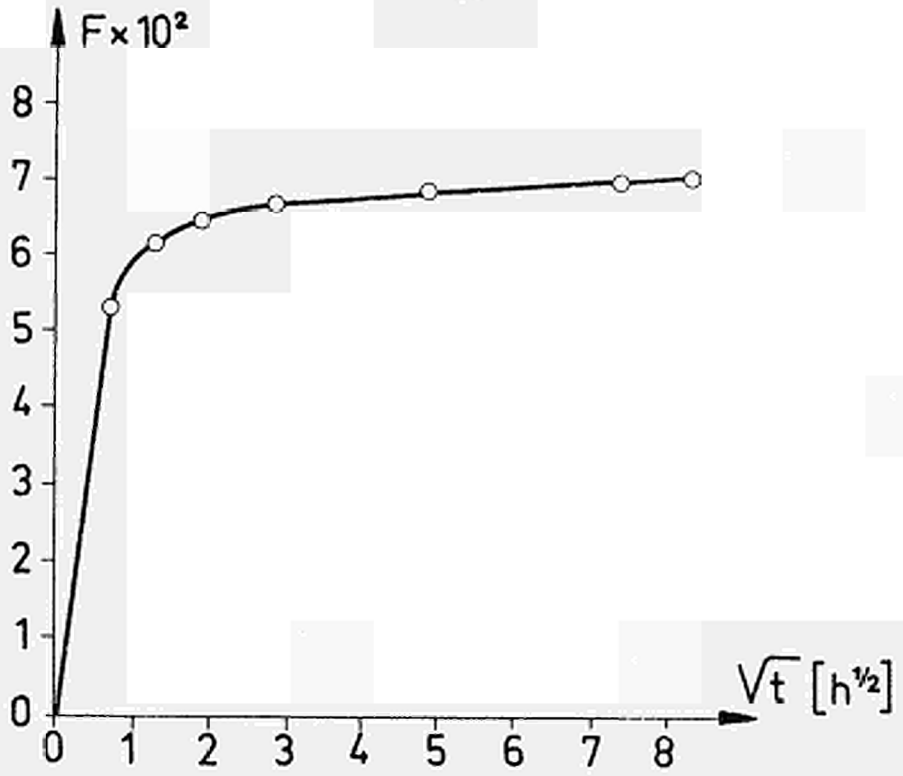

Fig. 1: Release of Xe-133 from UC powder at 1600°C (Schmeling, unpublished)

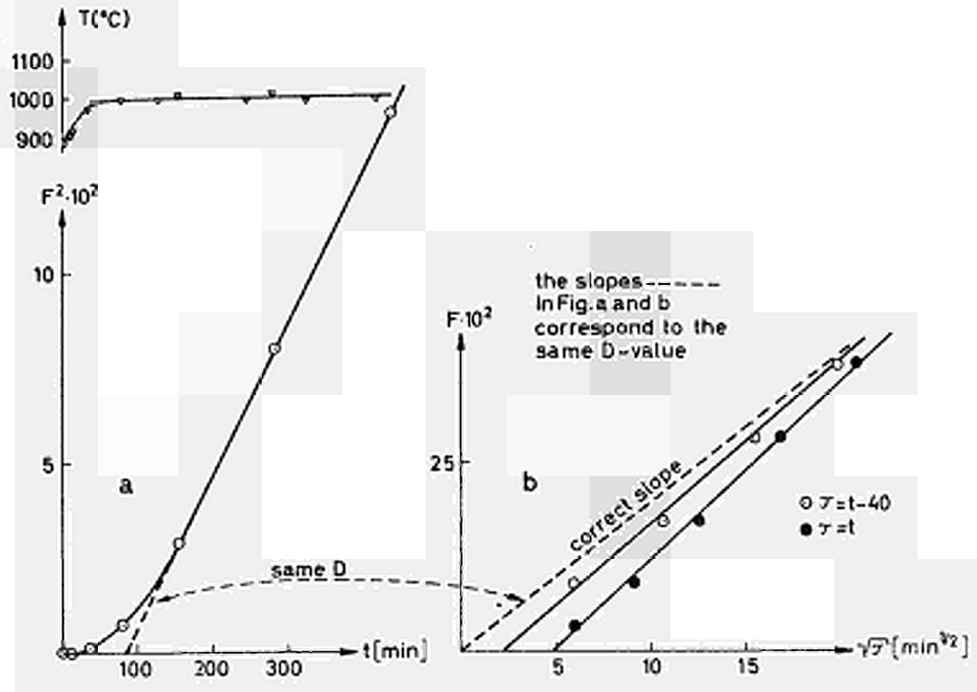

Fig. 2: Temperature variations, especially at the beginning of the anneal, can be taken into account for in an F^2-t-diagram; but not in an F-$\sqrt{t}$-diagram [CaF_2/Ar, Lagerwall, unpublished]

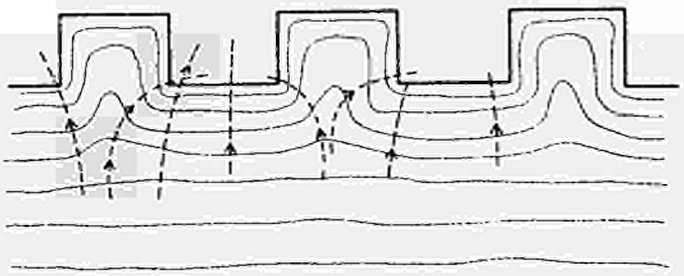

Fig. 3: Concentration potential and gradient near a simplified rough surface after a certain time has elapsed from the beginning of the anneal

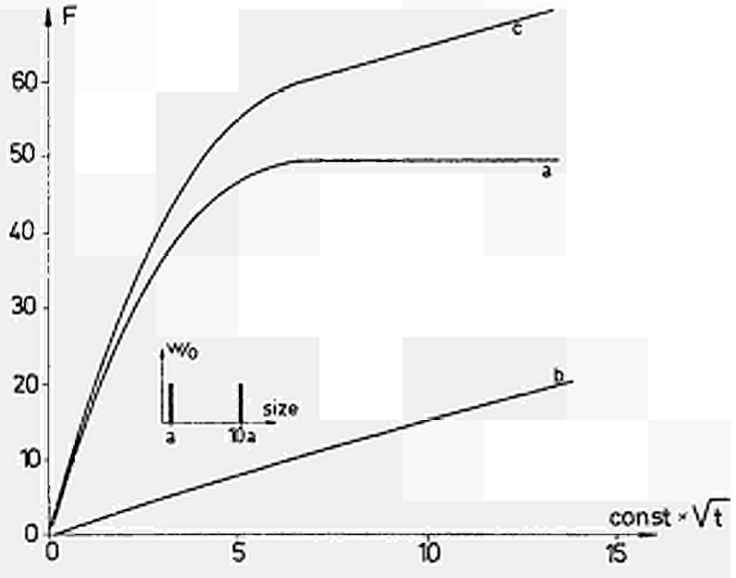

Fig. 4: Ideal release from a powder made up of only two particle sizes. The small particles are quickly emptied (a), the larger particles give curve (b); the observed curve is the sum of the two (c).

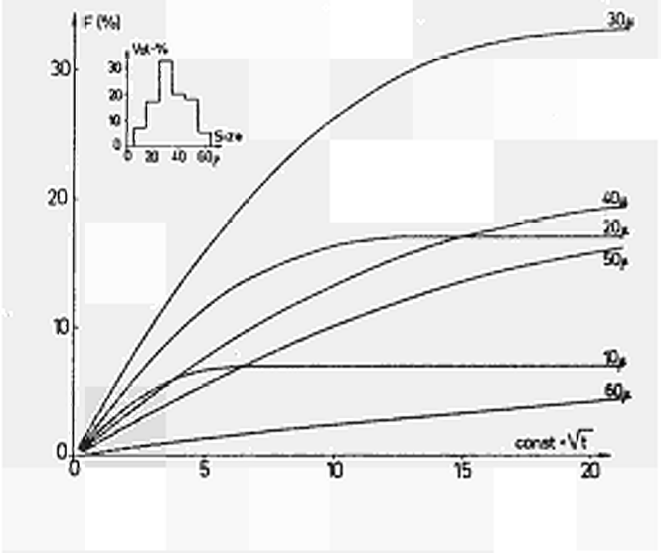

Fig. 5: Ideal release from UO_2 powder together with the corresponding grain size distribution

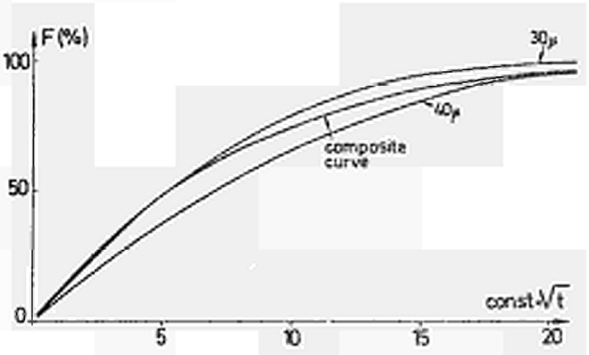

Fig. 6: The corresponding composite curve together with curves in case of powder made up of only 30 μ and 40 μ particles

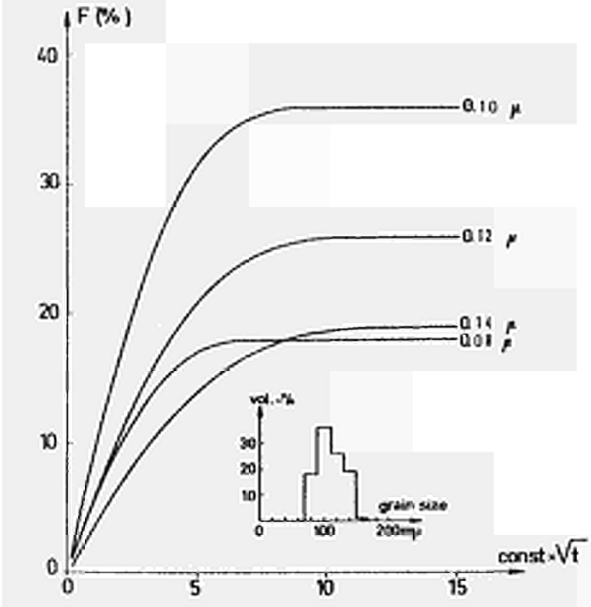

Fig. 7: Ideal release from UO_2 powder together with the corresponding grain size distribution

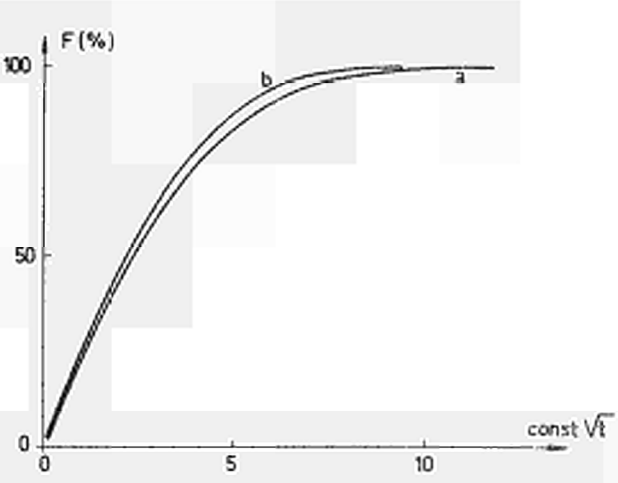

Fig. 8: The corresponding composite curve (a) together with curve in case of a powder made up of only 0.10 μ particles(b)

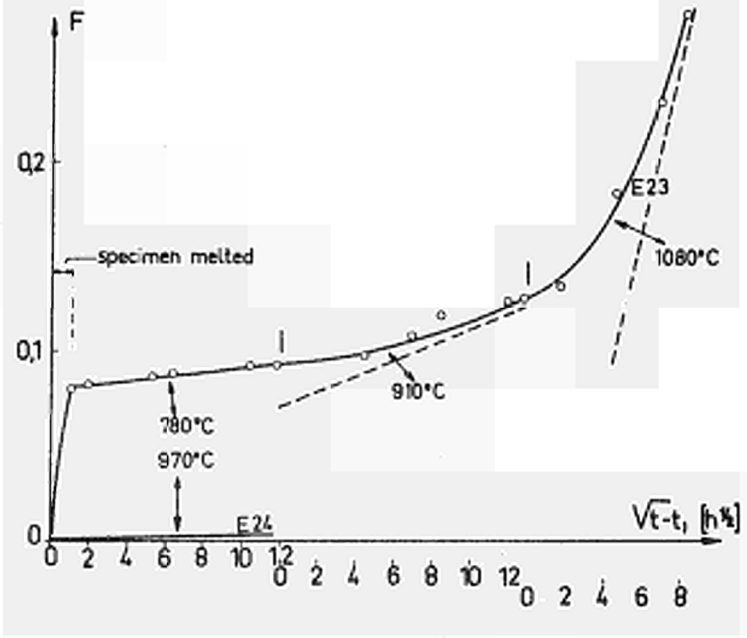

Fig. 9: Release of xenon from uranium metal, which had been melted for a short time after irradiation (curve E 23). Curve E 24 shows the release from a specimen which has not been melted before the PAD experiment [Schmeling, unpublished]

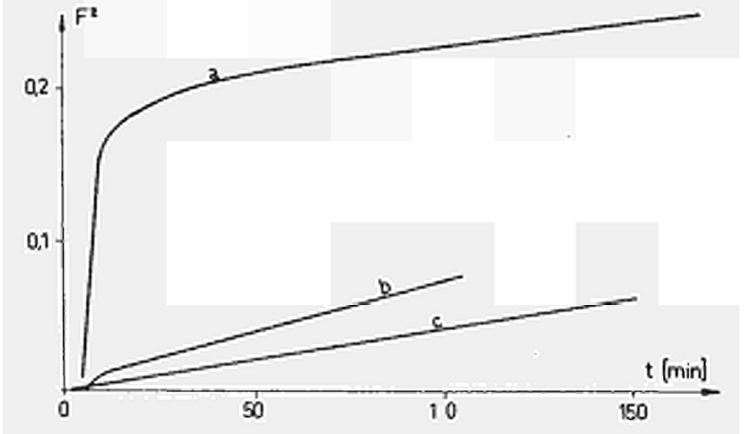

Fig. 10: Release of argon from pressed pellets of potassium fluoride. A pellet which is not preheated exhibits a pronounced burst (a); a preheated pellet a small burst only (b), and the subsequent release is similar to that from single crystal KF(c). [Mundt, unpublished]

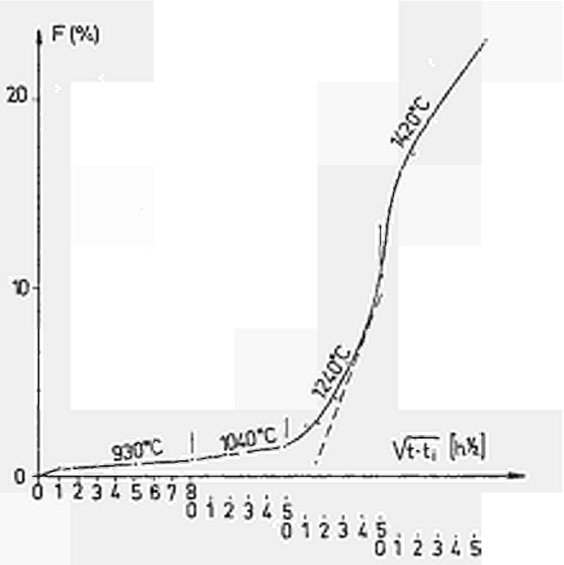

Fig. 11: Release of xenon from UC powder. The burst at 1420°C is supposed to be caused by a slight sintering of the powder particles. [Schmeling, unpublished]

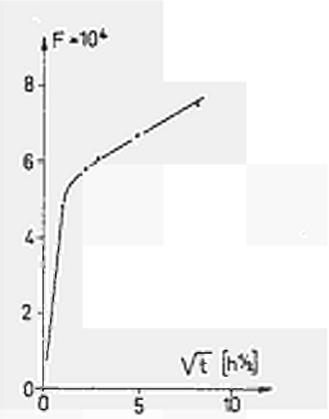

Fig. 12: Typical release of xenon from uranium metal during a vacuum anneal at about 970°C. The specimen was in contact with quartz, and was visually corroded after the run [Schmeling, unpublished]

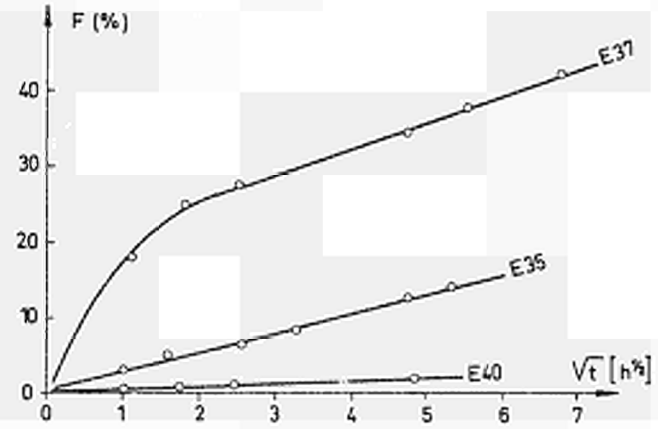

Fig. 13: Release of xenon from UC; the specimen in contact with alumina (E 37), with zirconia (E 35), and with tantalum (E 40). All experiments at 1410-1430°C [Schmeling, unpublished]

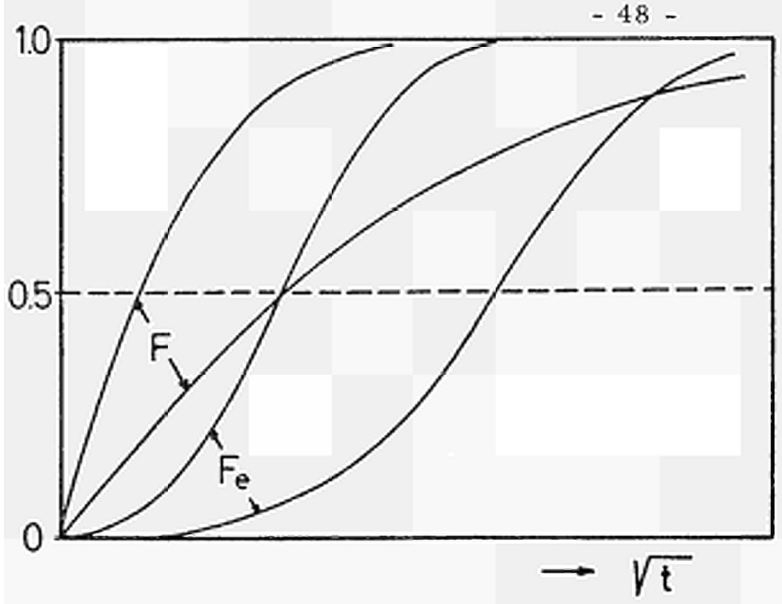

Fig. 14: Comparison between pure diffusion (F) and pure evapuration (F_e) kinetics. Note that diffusion ought to be predominant at the beginning. At t=0, the slope of F_e is zero, but that of F finite. In the corresponding F_e-t-diagram the slope of F_e is finite and that of F infinite large at t = 0.

Fig. 15: Release kinetics of argon in calcium fluoride. If the release is only due to volume diffusion in the lattice, the function φ^2 should be identical with the tangent at $F^2 = 0$, T = const. [10, 12]. The diffusion coefficient is obtained directly from the slope of φ^2: $D = \frac{2}{\sqrt{\pi}} \cdot \frac{S}{V} \frac{d\varphi^2}{dt}$. Though evaporation was observed at the high temperature stages in a and c, the diffusion seems to be perfectly undisturbed. The deviation in b corresponds to a decrease of S/V by evaporation. D can be accurately calculated from the slope of φ^2 extrapolated to $\varphi^2 = 0$.

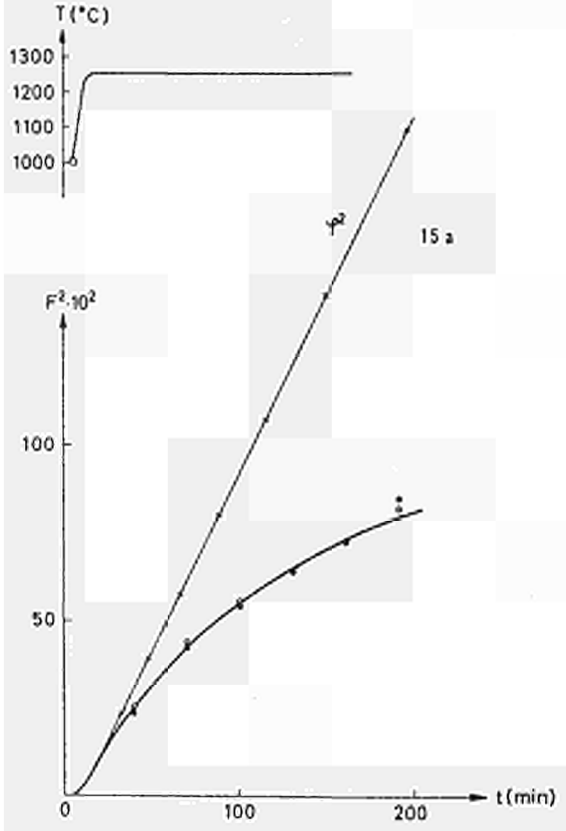

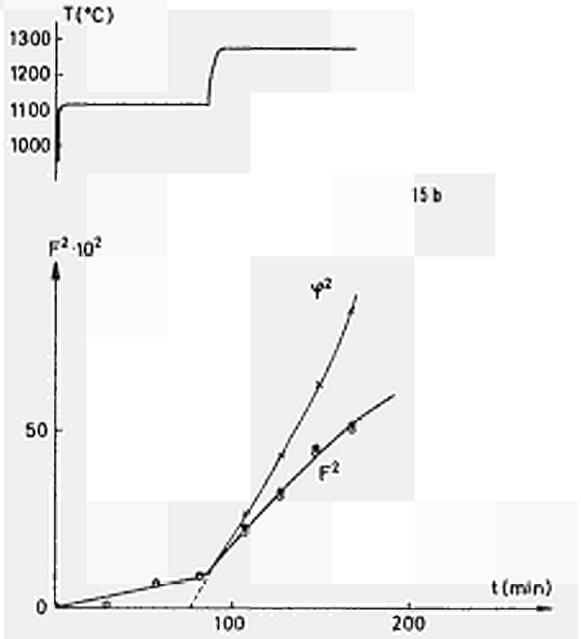

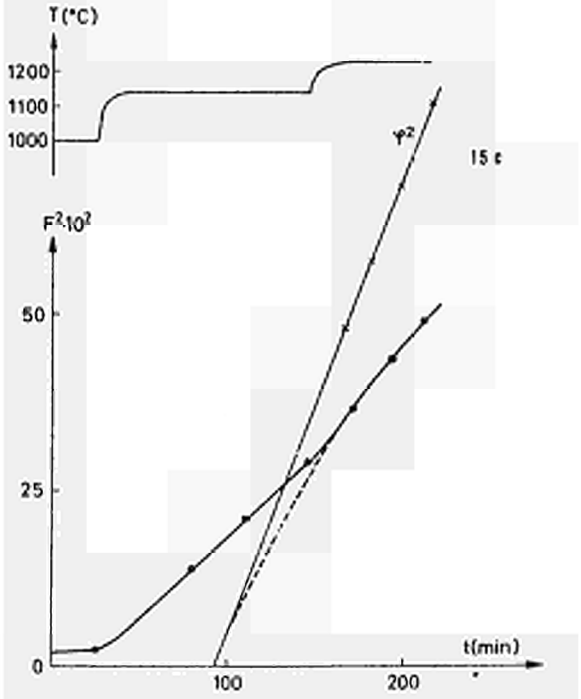

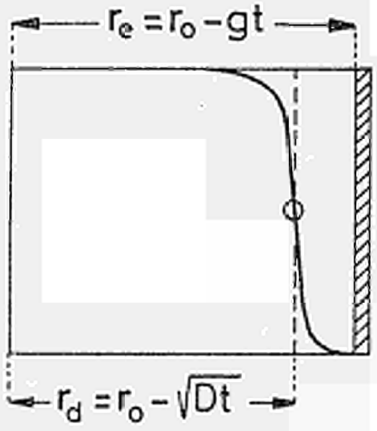

Fig. 16:
The concentration profile in a sphere with the initial radius r_0 after the time t has elapsed from the beginning of the anneal.

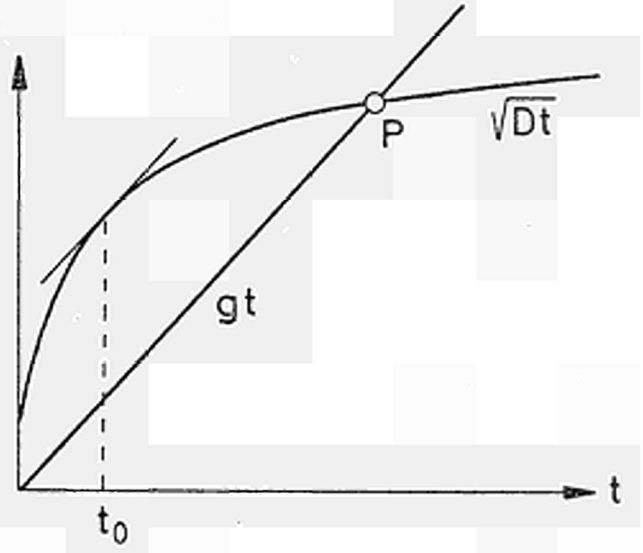

Fig. 17: The distances covered by the diffusion front and the evaporation front according to figure 16 at the time t.

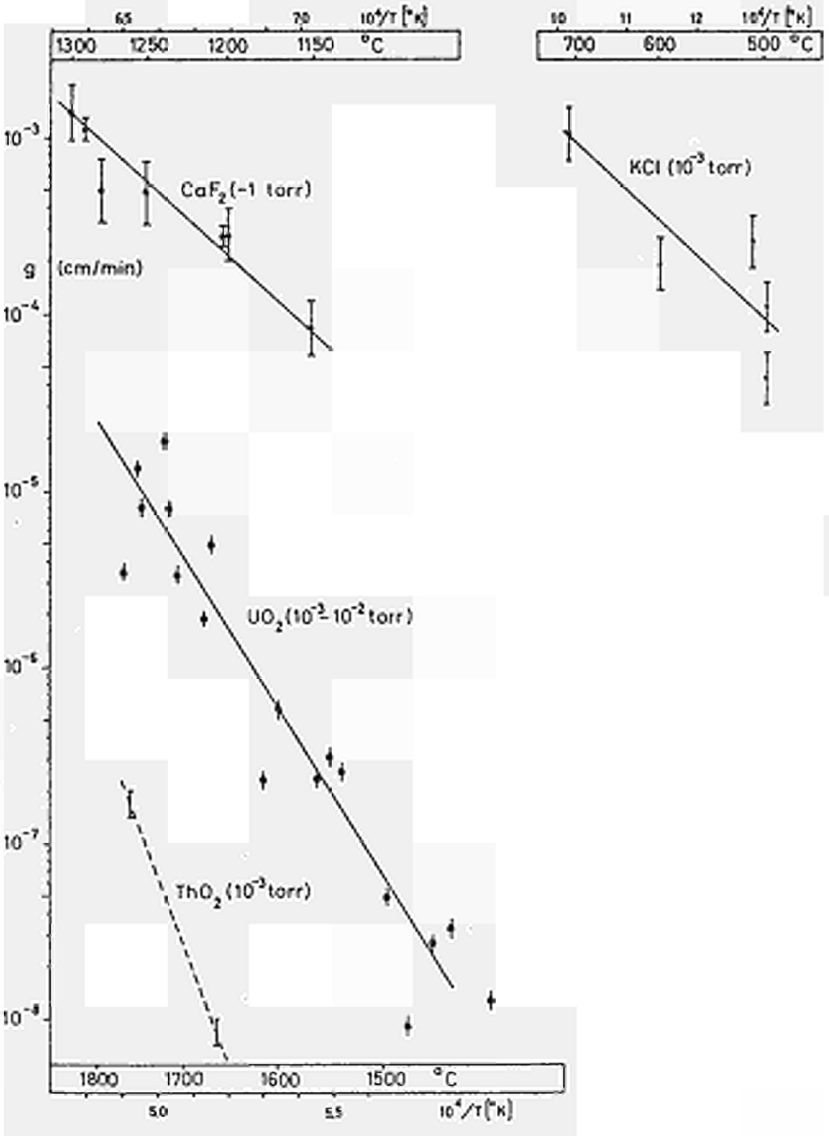

Fig. 18: The experimentally determed values of the quantity g in equation (5-1) as a function of temperature for different crystals.

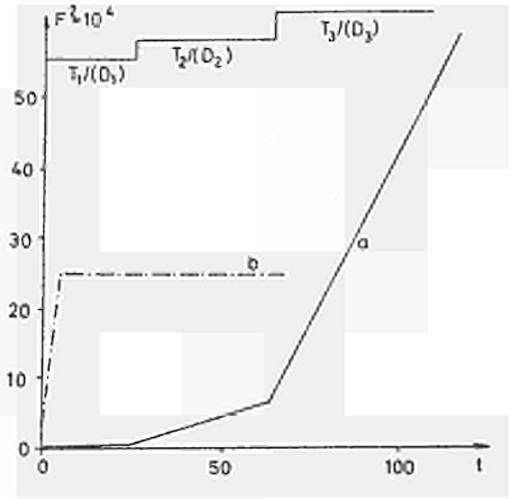

Fig. 19: Hypothetical example of release discussed in the text and used in several figures below: pure volume diffusion (curve a) and simultaneous release from other source (curve b)

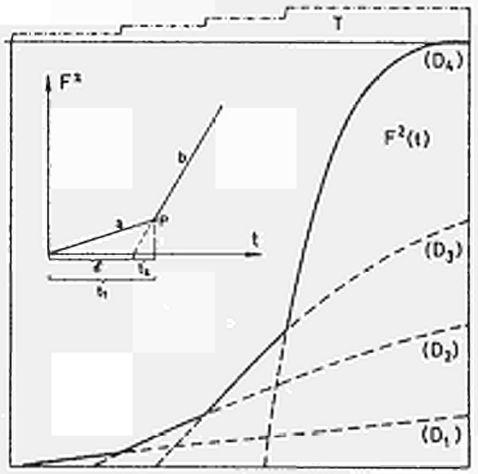

Fig. 20: The general behaviour of $F^2(t)$ in the case of undisturbed volume diffusion. The temperature is suddenly changed three times during the experiment, cf. explanations in the text.

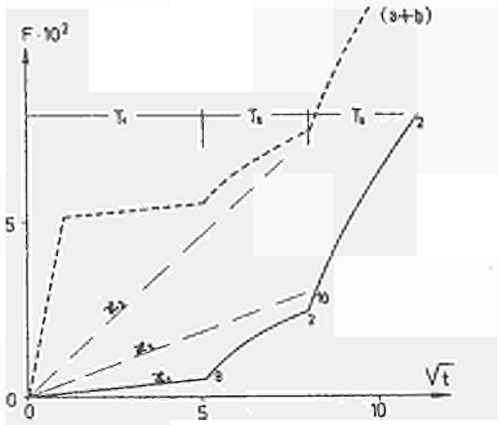

Fig. 21:

$F(\sqrt{t})$ plot of pure volume diffusion in case of multitemperature anneal (the same release as in fig. 19, curve a). The T_2- and T_3-branches simulate too high a diffusion coefficient and exhibit small bursts. The real values of D are given by the asymptotes. The small figures indicate how many times larger the simulated values of D are, compared with the real ones.

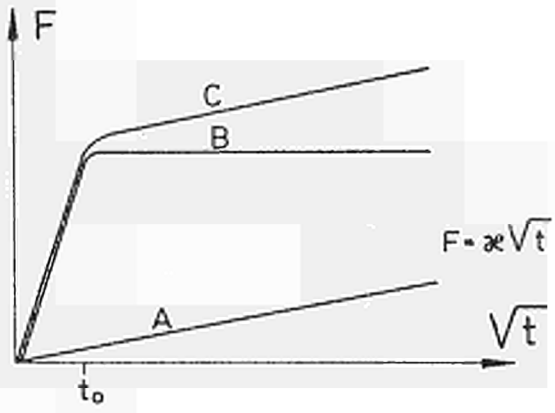

Fig. 22: $F(\sqrt{t})$-plot of pure volume diffusion(curve A) overlapped by another gas releasing process (curve B), resulting in a composite release (curve C).

Fig. 23: Ideal release superimposed by one single burst at the beginning of the anneal. (F-a+b from fig. 19). The branches at T_2 and T_3 are distorted in the F^2-t diagram because of the mere presence of the burst at T_1. The slope gives an incorrect D value for all three temperatures.

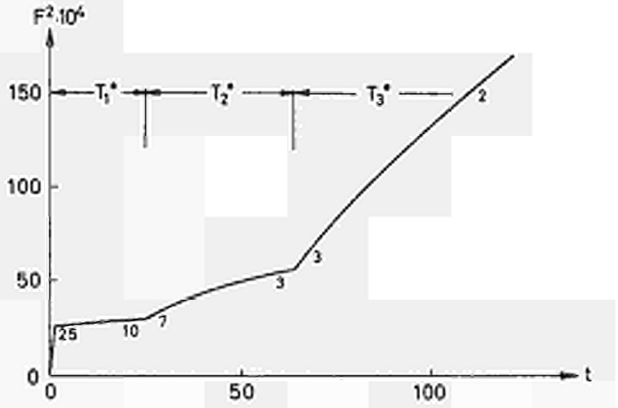

Fig. 24: The same case as illustrated in fig. 23, but plotted F vs $\sqrt{t-t_i}$.

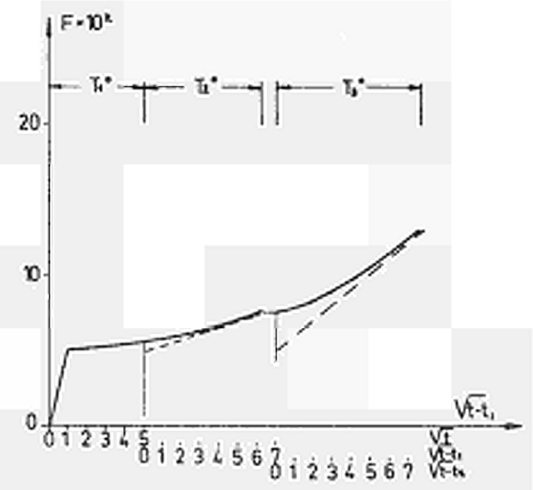

Fig. 25: Plot of F vs $\sqrt{t-t_i}$ for the case of an initial burst at the temperature T_1 and a second, smaller burst at T_2. No burst at T_3.